

Supplemental materials for

Morphological features and water solubility of iron in aged fine aerosol particles over the Indian Ocean

5 Sayako Ueda¹, Yoko Iwamoto², Fumikazu Taketani³, Mingxu Liu¹, Hitoshi Matsui¹

¹ Graduate School of Environmental Studies, Nagoya University, Nagoya, 464-8601, Japan

² Graduate School of Integrated Sciences for Life, Hiroshima University, Hiroshima University, Higashi-Hiroshima, 739-8521, Japan

³ Japan Agency for Marine–Earth Science and Technology, Yokohama, 237-0061, Japan

10 *Correspondence to:* Sayako Ueda (ueda.sayako.u2@f.mail.nagoya-u.ac.jp)

S1 Estimation of the water-soluble Fe fraction

For this study, the fraction of water-soluble Fe to total Fe in individual Fe-containing particles is estimated based on detected values of X-ray counts for Fe and Pd before and after water dialysis. The X-ray count sensitivity when detected using an EDS analyzer depends on the analytical conditions, such as the frame number for analyses and adjustment of the electron beam and detector. Because some conditions can change, evaluating X-ray count values as absolute values is difficult for samples analyzed on different days or at different settings. Although estimating the mass of each element is not possible, analyzing EDS spectra using software can estimate the mass fraction (MF) of each element from measurement results of X-ray counts as relative values to the selected elements. The mass fraction of element X can be calculated as shown below.

$$MF_X = \frac{m_X}{m_{total}} \quad (1)$$

Therein, m_X and m_{total} respectively represent the mass of an element X in a selected area and the mass of all analyzed (selected) elements in the area. For this study, TEM samples before water dialysis were coated uniformly by Pd/Pd using the shadowing method. Pd is not included in general aerosols. Therefore, the MF_X value standardized by MF_{Pd} , X/Pd , can be treated as an independent value from m_{total} , which changes according to the aerosol composition, collodion film thickness, and distance from the Cu grid.

$$X/Pd = \frac{MF_X}{MF_{Pd}} = \frac{m_X}{m_{Pd}} \quad (2)$$

Because Pd is a water-insoluble material coated onto the top surface on samples in this study, the mass of Pd for a selected area after water dialysis (m_{Pd_after}) can be regarded as equivalent to that for the same area before water dialysis (m_{Pd_before}).

$$m_{Pd_before} = m_{Pd_after} \quad (3)$$

The fraction of water-insoluble Fe (WIFe) mass to the total Fe mass in a particle, f_{WIFe} , can be represented as

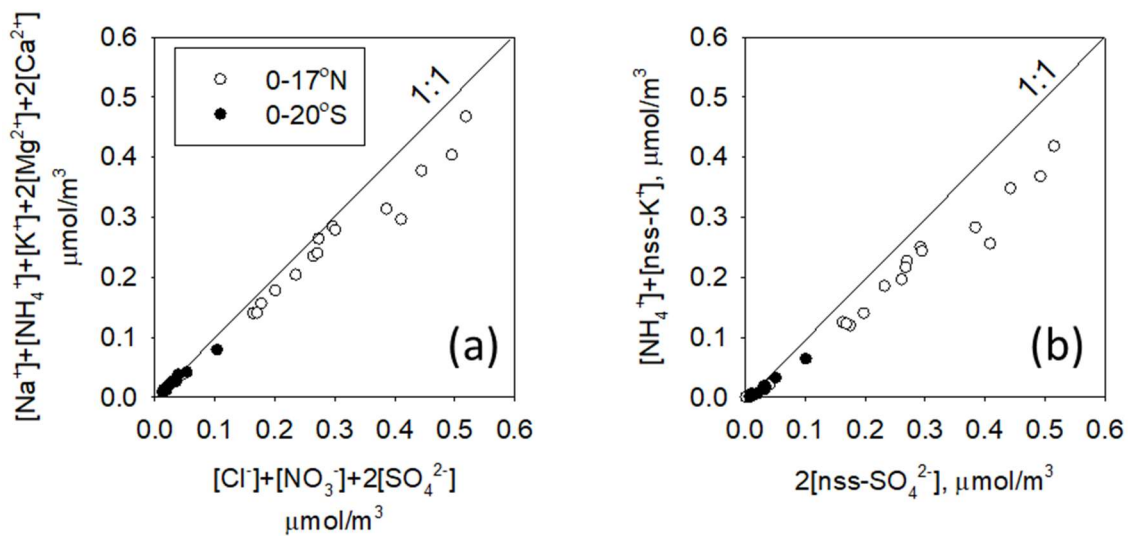
$$f_{WIFe} = \frac{m_{WIFe}}{m_{Fe}} \times 100 [\%] = \frac{m_{Fe_after}}{m_{Fe_before}} \times 100 [\%], \quad (4)$$

where m_{Fe_before} and m_{Fe_after} respectively denote the Fe mass before and after water dialysis for a Fe-containing particle. Under equation (3), equation (4) can be described using Fe/Pd before and after water dialysis of the same area for a Fe-containing particle (respectively, Fe/Pd_{before} and Fe/Pd_{after}), which are based only on measurable values.

$$f_{WIFe} = \frac{Fe/Pd_{after}}{Fe/Pd_{before}} \times 100 [\%] \quad (5)$$

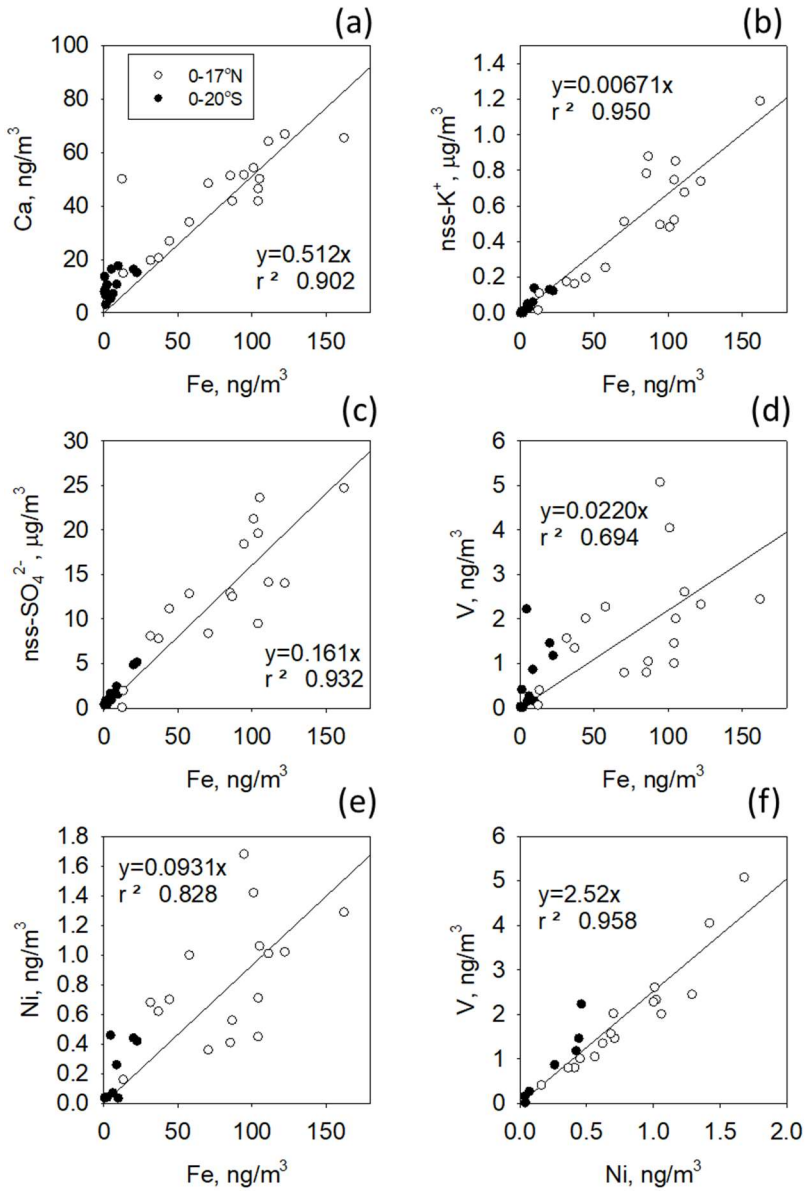
Finally, the fraction of water-soluble Fe to total Fe in a particle, f_{WSFe} can be estimated as presented below.

$$f_{WSFe} = 100 - f_{WIFe} [\%] \quad (6)$$



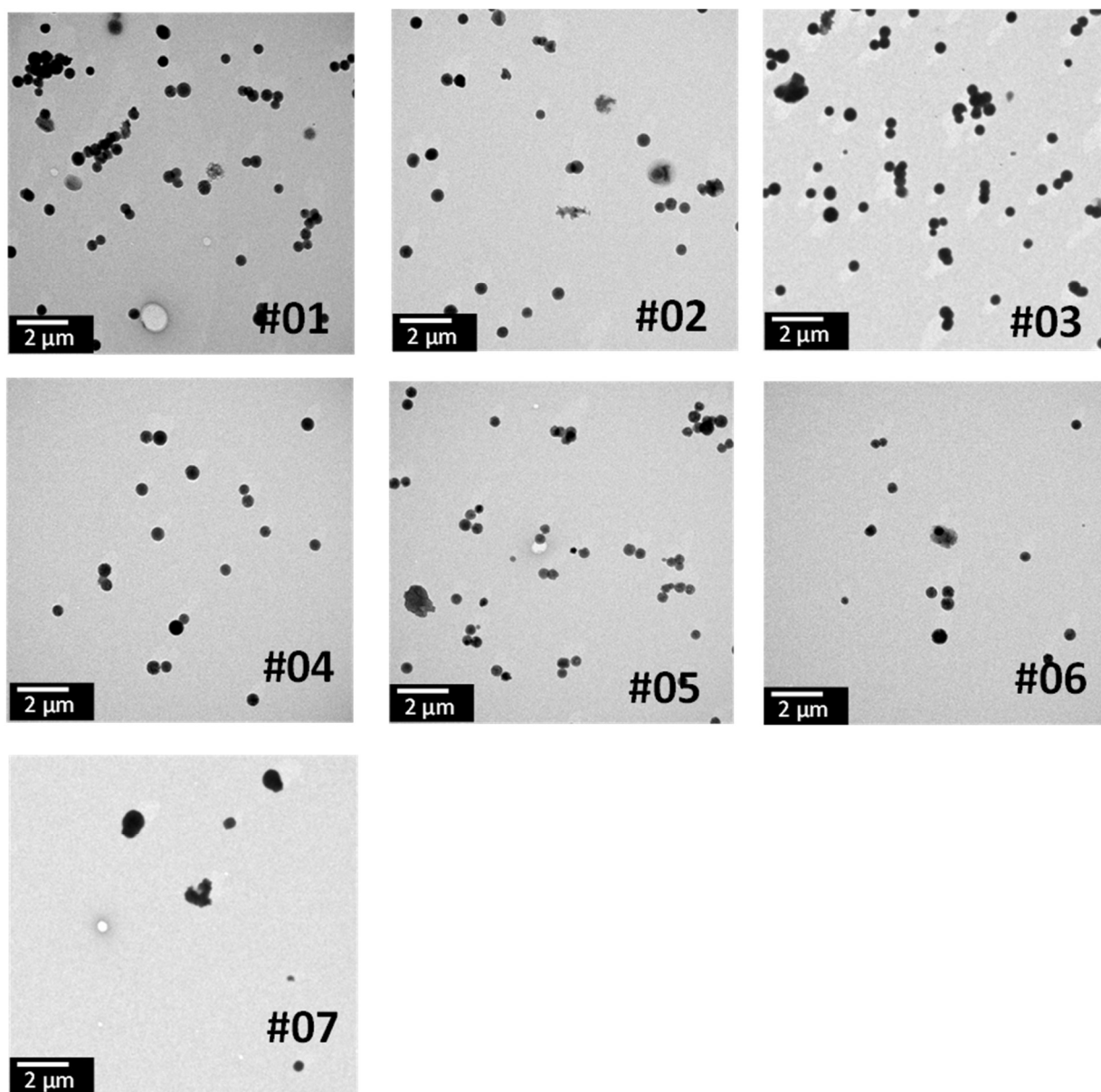
45

Figure S1: Scatter plots of (a) measured cation and anion amounts and (b) nss-SO₄²⁻ and NH₄⁺ plus nss-K⁺ amount in equivalent concentrations. Black circles and white circles respectively represent data for samples south and north of the equator.



50

Figure S2: Scatter plots of Fe to (a) Ca, (b) nss-K⁺, (c) nss-SO₄²⁻, (d) V, and (e) Ni mass concentrations and (f) scatter plots of V and Ni mass concentrations. Black circles and white circles respectively represent data for samples south and north of the equator. The fitting line is linearized for all dots.



55

Figure S3: Electron micrographs for (a) samples #01–07. All micrographs have equal magnification.

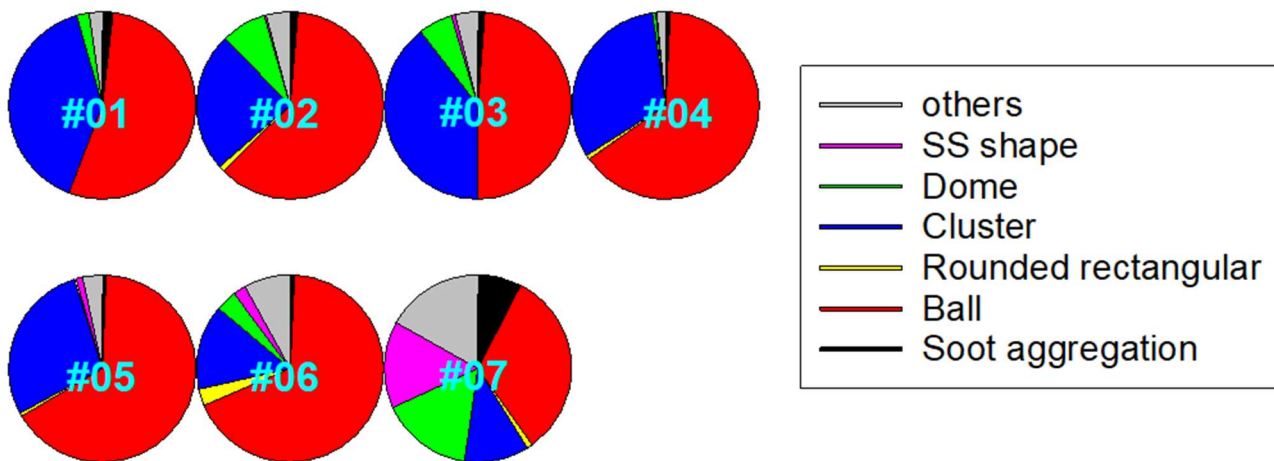
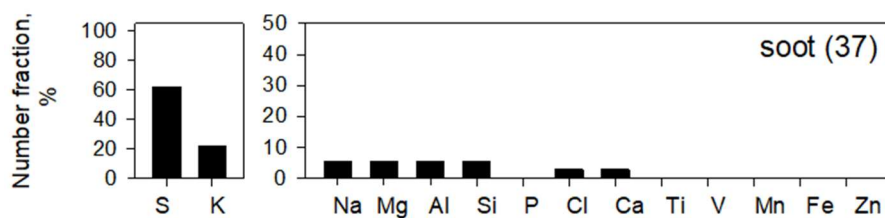
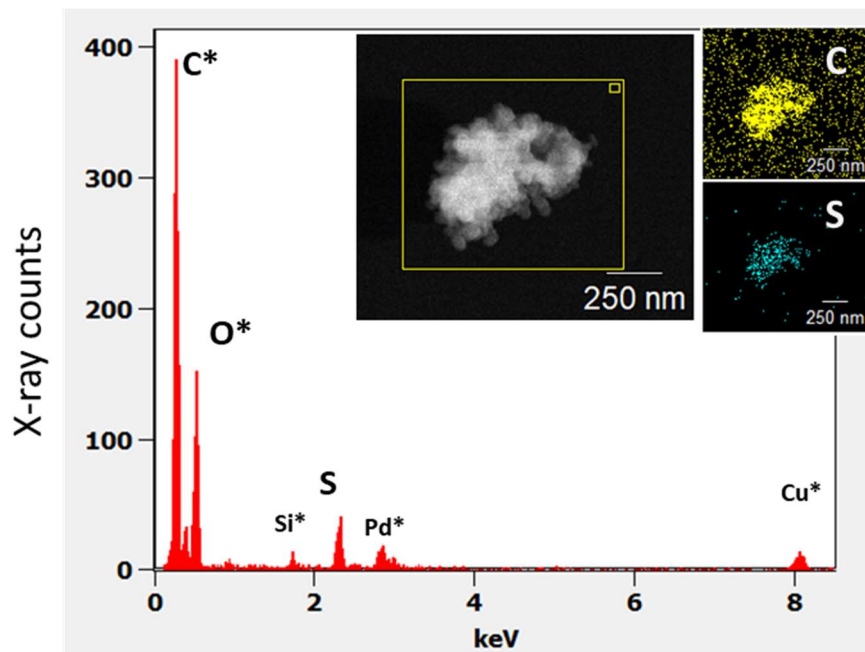


Figure S4: Pie chart showing number fractions of morphological types. The main text describes each morphological type feature.



65 Figure S5: Extracted X-ray count spectrum, STEM image and elemental map of soot particle (upper) and number fraction of each-element-containing particles in soot particles (lower). X-ray spectra were extracted from areas surrounded by yellow rectangles of the same size. Elements marked with asterisks include the background.

Table S1: Number of Fe-containing particles by type

Sample ID	Fe sphere in metal (spherical fly ash)		Fe with Si, Al or Ca heterogeneously (mineral dust)	FeO _x aggregation	Other shaped Fe	Small Fe thickly coated by sulfate
	in Si or Al	without Si and Al				
#01	0	0	1	0	0	2
#02	0	0	0	1	0	1
#03	4	0	2	1	1(1)*	9
#04	5	0	1	1(1) *	1	2
#05	0	2	2(1) *	0	1(1) *	5
#06	0	0	0	0	0	2
#07	0	0	0	0	0	1

70 * Numbers in brackets signify the number of bare type (without sulfate) Fe-containing particles